Available online at www.sciencedirect.com

ScienceDirect

Procedia Engineering 84 (2014) 306 – 319

Procedia Engineering

www.elsevier.com/locate/procedia

"2014 ISSST", 2014 International Symposium on Safety Science and Technology

Effects of obstacle separation distance on gas explosions: the influence of obstacle blockage ratio

Abdulmajid M. NA'INNA[a]*, Herodotos N. PHYLAKTOU[b], Gordon E. ANDREWS[b]

[a]*Armament Engineering Department, Air Force Institute of Technology, PMB 2104 Kaduna, Nigeria*
[b]*Energy Ressearch Institute, University of Leeds, Leeds LS2 9JT, United Kingdom*

Abstract

Obstacle separation distance (pitch) has received little systematic study in the literature. Either too large or small spacing between obstacles would lead to lesser explosion severity. Therefore, an optimum value of the pitch that would produce the highest flame acceleration and hence overpressure is needed. It was the aim of this work to investigate the influence of obstacle blockage ratio on the obstacle spacing in gas explosions. The explosion tests were performed using methane-air (10% by vol.), in an elongated vented cylindrical vessel 162 mm internal diameter with an overall length-to-diameter, L/D of 27.7. Double 20-40% blockage ratio, BR orifice plates were used as obstacles. The spacing between the obstacles was systematically varied from 0.5 m to 2.75 m. The 40% BR produced the highest explosion severity in terms of overpressure and flame speeds when compared to 30% and 20% BR. However, the worst case obstacle spacing was found to be shorter with increase in obstacle blockage. In general, similar profiles of overpressures and flame speeds were obtained for all the obstacle blockages. This trend was equally observed in the cold flow turbulence intensity profile generated behind a grid plate by other researchers. In planning the layout of new installations, the worst case separation distance needs to be avoided but incorporated when assessing the risk to existing set-ups. The results clearly demonstrated that high congestion in a given layout does not necessarily imply higher explosion severity as traditionally assumed. Less congested but optimally separated obstructions can lead to higher overpressures.

Peer-review under responsibility of scientific committee of Beijing Institute of Technology

Keywords: Gas explosion; obstacle; obstacle separation distance; turbulence intensity

* Corresponding author. Tel.: +2348030679898; fax: +0-000-000-0000 .
E-mail address: amnainna@gmail.com; pm08amn@leeds.ac.uk

Peer-review under responsibility of scientific committee of Beijing Institute of Technology
doi:10.1016/j.proeng.2014.10.439

Nomenclature

b	obstacle scale
BR	blockage ratio
d	orifice diameter
D	tube diameter
L/D	length to diameter ratio of a tube
M	mesh length
P_{max}	maximum overpressure
S_{fmax}	maximum flame speed
S_{fu}	upstream flame speed
S_g	gas velocity
t	obstacle thickness
t/d	aspect ratio
u′	r.m.s velocity
U	mean flow velocity
u′/U	intensity of turbulence
x	axial distance
x/b	distance downstream of a grid
x_s	obstacle separation distance
x_s/b	dimensionless obstacle separation distance
$(x/b)_{max}$	position to maximum intensity of turbulence
1	effects due to first obstacle
2	effects due to second obstacle

1. Introduction

1.1. Review on congested gas explosions and obstacle spacing

In congested gas explosions typically found in process industries, the spacing between obstacles (pitch) is one of the parameters (among others e.g. blockage ratio, number, size, shape etc.) that affects the severity of such explosions. However, there is limited knowledge on the influence of this parameter in the gas explosions literatures. Sustained flame acceleration could not be attained for large pitch due to decay of turbulence in between obstacles while for small pitch the pocket of unburned gas between the obstacles would be too small to allow for the flame to accelerate before reaching the next obstacle [1]. In between there has to be a worst case explosion interaction obstacle spacing and there is no previous work that determines this. In compliance with the ATEX directive [2], the worst case scenarios need to be used in assessing the severity of the hazard posed by gas explosions in process plant or offshore oil and gas platforms. In planning the layout of new installations, it is appropriate to identify the relevant worst case obstacle separation in order to avoid it. In assessing the risk to existing installations and taking appropriate mitigation measures it is important to evaluate such risk on the basis of a clear understanding of the effects of separation distance and congestion.

Most researchers conducted gas explosion experiments with multi-obstacle arrays but with no variation in obstacle separation distance [3-22].The influence of obstacle separation distance on gas explosion severity from the above experiments could not be quantified because of the fixed pitch that was used within each set of experiments. With the exception of [13,17], the pitch in all of the above studies was varied just from 1.2 to 8.8 characteristic obstacle scales. However, this is not within the range of 3 to 20 characteristic obstacle scales downstream of the grid where the maximum combustion rate usually occurs as given by [23].

A number of experimental explosion studies have demonstrated the effect of obstacle separation distance as part of wider assessment of the effects of congestion [24-41]. The bulk of the spacing between obstacles was short and just within a range of 1.3 to 10 obstacle scales. Also; the justification to spacing of obstacles in most of the studies was not given by the researchers.

In most cases many repeat obstacles were used over a short distance and in some tests the pitch was varied over limited range for example [26,28,30,38]. In [42] the obstacle set-up in the form of 3D tube lattices could be regarded as a single porous structure. Also, there have been a number of investigations in explosions in obstacle-laden tubes where the separation distance of the multi-obstacles was also partially explored [31-34,37,38,41]. In most of the tests, the explosion geometry was filled completely with obstacles thereby leading to deflagration to detonation transition, DDT.

Most of the industrial explosion incidents involved deflagrative rather than detonative propagation, and it is important therefore to explore the influence obstacle separation in scenarios where the combustion remains in the deflagration regime without transition to detonation.

The authors [43] reported an experimental study in an elongated tube with two obstacles with 30% area blockage, where the obstacle separation distance was varied systematically from 0.5 m to 2.75 m. They reported a direct influence of the obstacle separation distance on flame speed and overpressure. A separation distance of 1.75 m produced close to 3 bar overpressure and a flame speed of about 500 m/s with 10% methane/air explosions. These values were of the order of twice the overpressure and flame speed with a separation pitch of 2.75 m. The profile of effects with separation distance agreed with that of turbulence profile determined in **cold flows** as shown in Fig. 1.

Also, the authors [44] investigated the influence of mixture reactivity and fuel type on the optimum obstacle separation distance for generation using two induced turbulent generating orifice plates of 30% blockage with variable obstacle spacing.

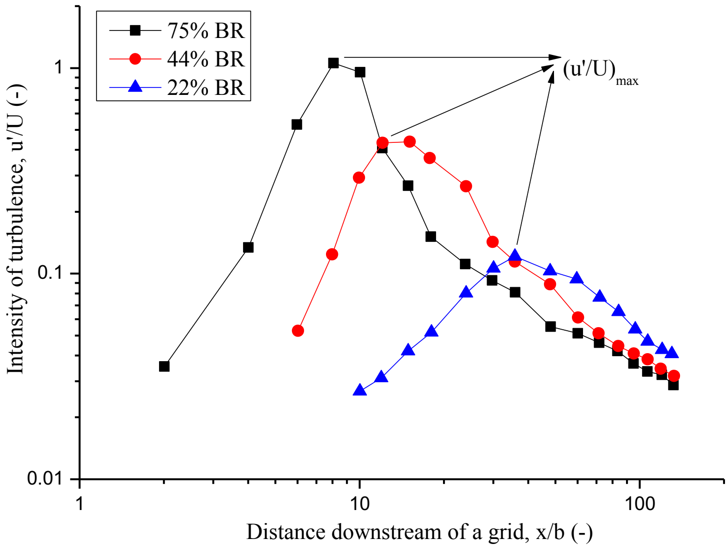

Fig. 1. Turbulence intensity downstream of grid-plates of various obstacle blockages [43].

It was the aim of this work to extend the investigation into the influence of obstacle spacing and blockage ratio on two obstacles with a view to obtaining the worst case obstacle spacing corresponding to maximum explosion overpressures.

1.2. Prediction of position to maximum intensity of turbulence

The interaction of the explosion induced unburnt gas flow with obstacles results in the generation of turbulence downstream of the obstacle and the acceleration of the flame when it reaches this turbulence. Extremely fast explosion flames can be generated by this mechanism giving rise to severe overpressures. Understanding and prediction of these phenomena is of concern to process industries, and in particular in assessing the risks and designing suitable protection and mitigation measures against vapour cloud explosions.

From Fig. 1, it is evident that there is an "optimum" spacing for obstacles where each successive obstacle is placed just after position of peak turbulence so that it "sees" the maximum flame speed. This would in turn be expected to cause the maximum possible turbulence downstream of that obstacle and therefore overall would cause the fastest possible acceleration to the highest possible flame speed and hence highest overpressure. Conversely if the obstacle spacing is larger or smaller than the optimum, then flame acceleration would not be as severe and the limit cases (too near or too far) the effect of repeat obstacles would be minimal.

The position to maximum intensity of turbulence, x_{max} has been correlated using the limited steady state experiments from [45-51].

The application of the steady state flows to the current experimental work (transient flows) is due to the inadequate experimental measurements of these turbulent flows in gas explosions due to transient nature of explosion flows and the connected harsh conditions. This technique has been applied by [52] who presented a method to estimate the maximum intensity of turbulence behind a grid plate obstacle by an explosion induced flow in terms of steady-state theory. Also, [53] applied steady state flows to perform a simple assessment methodology for vented explosions.

Figure 2 shows the relationship between the dimensionless distances to peak intensity, $(x/b)_{max}$ behind the grid against an obstacle blockage with an aspect ratio (t/d) of less than 0.6. The $(x/b)_{max}$ was found to increase with decrease in obstacle blockage. A power fit equation to the data is given as,

$$(x/b)_{max} = 2.77BR^{-1.55} \tag{1}$$

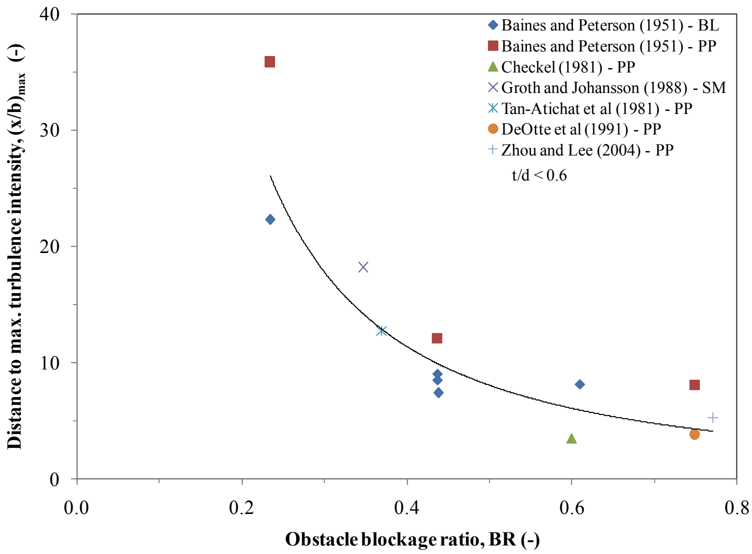

Fig. 2. Maximum intensity of turbulence against obstacle blockage from cold flow turbulence for t/d < 0.6.

In the present research, the developed model in Eq. 1 was used to guide the spacing between obstacles that would lead to maximum intensity of turbulence and thus severe explosion overpressures.

2. Experimental set-up

An elongated cylindrical vessel 162 mm internal diameter made from nine flanged sections, 8 of them of 0.5 m length each and one section 0.25 m in length (total nominal length of 4.25m). The test vessel was rated to withstand an overpressure of 35 bar. The test vessel was mounted horizontally and closed at the ignition end, with its open end connected to a large cylindrical dump-vessel with a volume of 50 m^3. This arrangement enabled the simulation of open-to-atmosphere explosions with accurate control of both test and dump vessels pre-ignition conditions.

Two orifice steel plate obstacles of 3.2 mm thick, and 20-40% blockage were used in the test vessel. The obstacle scale (b = 24 – 43 mm) was considered to be the nominal width of the solid material between holes using the same definition given in [45] for multi-hole grids, based on notional large grid plate with multiple holes of size and blockage ratio equal to the single hole actual obstacle, given as,

$$b = M - 0.95d \quad (2)$$

The obstacles were mounted between the section flanges. The first obstacle was positioned 1 m downstream of the spark (for all tests) while the second obstacle's position was varied from 0.5 m to 2.75 m downstream of the first obstacle.

A pneumatically actuated gate valve isolated the test vessel prior to mixture preparation. A vacuum pump was used to evacuate the test vessel before a 10 % (by vol.) methane-air mixture was formed using partial pressures, to a total mixture pressure of 1 atm. The dump vessel was filled with air to a pressure of 1 atm as well. After mixture circulation, allowing for at least 4 volume changes, the gate valve to the dump vessel was opened and a 16 Joule spark plug ignition was effected at the centre of the test vessel closed-end flange. The test vessel had an overall length-to-diameter ratio, L/D of 27.7. The set-up is shown in Fig. 3.

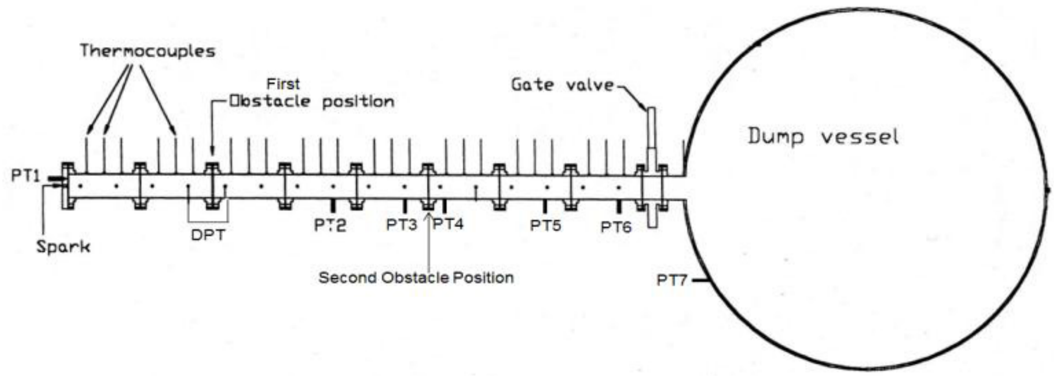

(a)

(b)

Fig. 3. Experimental set-up.(a) Schematic diagram, (b) Photograph.

An array of 24 type-K mineral insulated exposed junction thermocouples positioned along the axial centre line of the test vessel was used to record the time of flame arrival. Average flame speeds allocated to the midway position between two thermocouples were obtained by dividing the distance between two thermocouples by the difference in time of flame arrival at each thermocouple position. A smoothing algorithm was applied to the flame arrival data, as described by [17], to avoid either high or negative flame speeds where the flame brush appears to arrive at downstream centreline locations earlier than upstream ones, particularly in the regions of strong acceleration downstream of the obstacles.

The test vessel and dump vessel pressure histories were recorded using an array of 8 Keller-type pressure transducers - 7 gauge pressure transducers (PT1 to PT7) and 1 differential (DPT), as shown in Fig. 3. Wall static pressure tapping measured by a differential pressure transducer (DPT) were located at 0.5D upstream and 1D downstream of the first obstacle as specified by BS5167-2-2003. Pressure transducers, PT3 and PT4 were positioned 0.5D upstream and 1D downstream of the second obstacle and they were used to obtain the pressure differential across these obstacles. These were used in calculating the induced gas flow velocities and other flow turbulence characteristics (but these are not reported in this paper). Pressure transducers PT1 and PT6 were positioned permanently at the ignition position-end flange and end of the test vessel (25D from the spark) respectively. The pressure history in the dump vessel was measured using PT7 positioned as shown in Fig. 3.

A 32-channel (maximum sampling frequency of 200 KHz per channel) transient data recorder (Data Logger and FAMOS) was used to record and process the explosion data. Each test was conducted three times in order to demonstrate repeatability and ensure representative data and the average of the repeat tests was used for the analysis of the results.

Table 1 shows a summary of the tests carried out as part of this report and an overview of the results.

Table 1. Overview of experimental test conditions and results.

BR (-)	x_s (m)	b (m)	x_s/b (-)	S_{fu1} (m/s)	S_{fu2} (m/s)	S_{g1} (m/s)	S_{g2} (m/s)	P_{max} (bar)	S_{fmax} (m/s)
0	-	-	-	-	-	-	-	0.256	122
0.2	-	0.024	-	58	-	44	-	0.566	198
0.2	1.75	0.024	73	51	236	41	98	0.995	290
0.2	2.25	0.024	94	53	259	45	124	1.164	362
0.2	2.75	0.024	115	52	200	42	79	0.710	240
0.3	-	0.033	-	49	-	41	-	1.091	270
0.3	0.5	0.033	15	66	131	34	80	1.623	307
0.3	1.0	0.033	30	61	247	36	114	1.850	381
0.3	1.25	0.033	38	56	263	41	132	2.198	465
0.3	1.75	0.033	53	55	212	42	153	2.680	486
0.3	2.25	0.033	68	52	271	41	116	1.858	381
0.3	2.75	0.033	83	50	204	38	64	1.222	323
0.4	-	0.043	-	48	-	34	-	1.649	370
0.4	1.25	0.043	29	57	337	32	138	3.103	573
0.4	1.5	0.043	35	42	294	35	160	3.378	716
0.4	2.25	0.043	52	63	307	35	128	2.085	522

3. Results and discussions

3.1. Single obstacles

Figure 4 shows the relationship between the maximum overpressure against obstacle blockage for single obstacles. It was observed that the increase in obstacle BR resulted in increasing maximum overpressure. This could be attributed to the increase in obstacle scale with blockage from 24 mm, 33 mm and 43 mm for 0.2, 0.3 and 0.4 obstacle blockages respectively. The highest overpressure of about 1.7 bar from 0.4 BR obstacle was attained and this value was 1.5, 2.9 and 6.6 times greater than 0.3 BR, 0.2 BR and no obstacle tests respectively.

A similar trend was noticed from the previous studies of [25,27,35,54-55] among others. However, at high obstacle blockage (from 0.5 BR), the maximum overpressure was found to decrease with increasing blockage [13, 17]. The presence of such high blockages (small orifice diameter) prevented the flame from developing as freely as would have done without the obstacle. This caused the flame to develop faster radially and touch the vessel walls at a shorter distance from the spark.

Also shown in Fig. 4 is the relationship between the maximum flame speeds against obstacle blockage. Similar to maximum overpressure, a linear relationship was obtained. The highest flame speed (370 m/s) attained was with 0.4 BR. This value was a factor of 1.4 and 1.9 greater than 0.3 and 0.2 obstacle blockage ratios respectively.

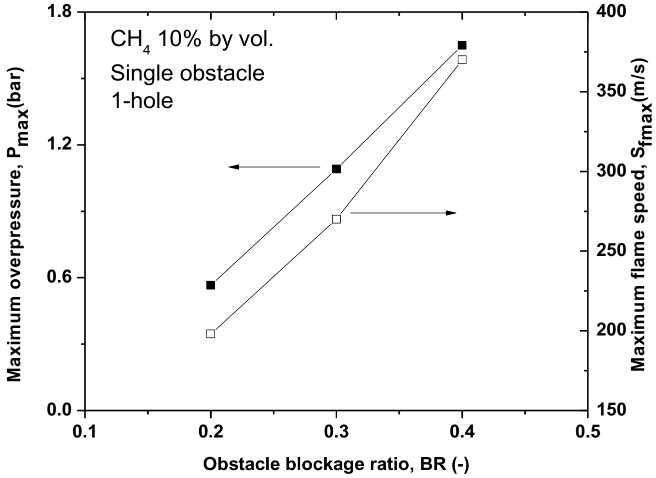

Fig. 4. Influence of maximum overpressure and flame speeds against obstacle blockage.

3.2. Double obstacle

Example pressure records from pressure transducer PT6 are shown in Fig. 5, for different obstacle separation distances with obstacles of 0.3 blockage ratio. The data clearly demonstrated a very strong effect of the obstacle separation distance not only in terms of the maximum pressure achieved but also in terms of the profile of the pressure development. For obstacles in close proximity to each other (e.g. 0.5 and 1.0m separation distances) the effect of the obstacles was amalgamated into one pressure rise whilst on the cases where the separation distances are too large (e.g. 2.75 m separation distance) the effects of the individual obstacles become distinct with no significant influence of the first obstacle on the flame behaviour after the second.

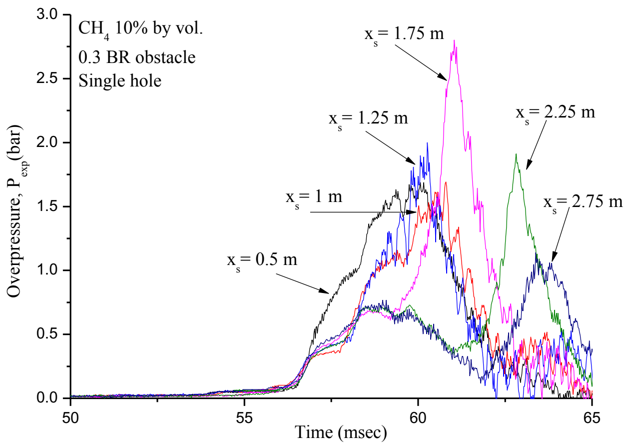

Fig. 5. Example pressure records from pressure transducer PT6, for different obstacle separation distances [43].

The maximum synergistic effect of the two obstacles was obtained at a separation distance of 1.75 m where evidently the flame accelerated to its maximum value after the first obstacle before reaching the second. Therefore the highest possible flows were induced by the accelerating flame through the second obstacle and this would have resulted in the highest turbulence levels after the second and hence to highest overpressures, as shown when the flame reached this region. This concept and behaviour is fully congruent with the turbulence profile downstream of an obstruction presented by [45].

The influence of maximum overpressure and flame speed against dimensionless obstacle spacing for various obstacle blockage ratios is shown in Fig. 6. A trend comparable to single obstacles was noticed with the double obstacle tests but with a higher magnitude of maximum overpressure. The highest overpressure produced with 0.4 BR was 3.4 bar which was 1.3 and 2.8 folds greater than 0.3 and 0.2 obstacle blockage respectively. However, the positions to such maximum overpressures were different with obstacle blockage. The higher obstacle 0.4 BR occurred at a shorter distance (34.9 obstacle scales) in comparison to 0.3 and 0.2 BRs which emerged at 52.7 and 92.4 obstacle scales respectively. This trend was similar to cold flow turbulence intensity of [45].

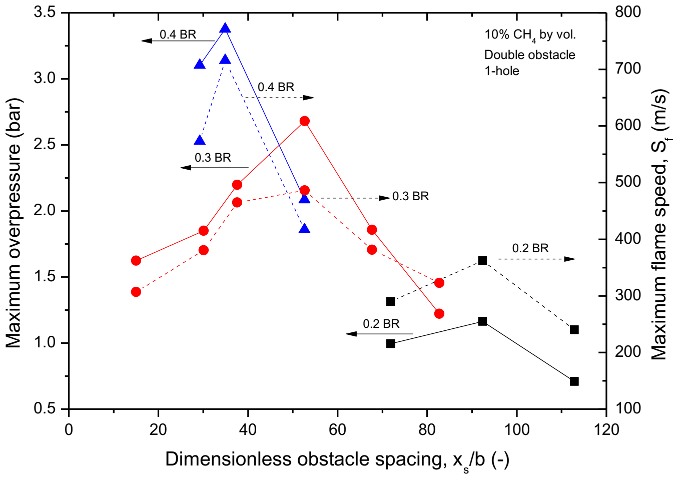

Fig. 6. Effect of explosion overpressure and flame speed on dimensionless obstacle spacing and obstacle blockage.

The positions to maximum overpressures and hence intensity of turbulence obtained for the 0.2-0.4 BRs in this work were in agreement with the cold flow prediction correlation of distance to maximum intensity of turbulence as given in Eq. 1 if multiplied by a factor of three.

For the double obstacle tests with variable obstacle spacing, the effect of obstacle blockage with maximum flame speeds is also given in Fig. 6. The highest peak flame speeds transpired with a BR of 0.4 followed by 0.3 and 0.2 in that order as 716 m/s, 486 m/s and 362 m/s. However, these values occurred at different obstacle spacing. A similar turbulence profile observed with maximum overpressure with dimensionless spacing was also discernible with the maximum flame speed.

The effectiveness of optimum obstacle spacing with just two obstacles with 0.2-0.4 blockage ratios (current work) was compared with the work of Moen *et al* .[25] using multi obstacles in a large scale vented elongated tube of 50 m^3. The obstacles in the large scale tests were 0.16-0.5 blockage and spaced 2 m apart. Fig. 7 shows the peak overpressure effect against obstacle blockage for small and large scale tubes using methane-air combustible mixtures.

Even though the obstacle BRs were not the same in both scenarios (with the exception of 0.3 BR), an increase in maximum overpressure and blockage was obtained with the larger scale from [25] been of higher magnitude than the present work. For 0.3 BR, the larger scale (50m^3 tube) produced nearly 4 bar overpressure which is only 1.5 times higher than the small scale in the current work (0.1 m^3 tube). This overpressure would have been greater if the obstacle spacing (2 m) was at its optimum which is going to be larger than 2 m based on Eq. 1.

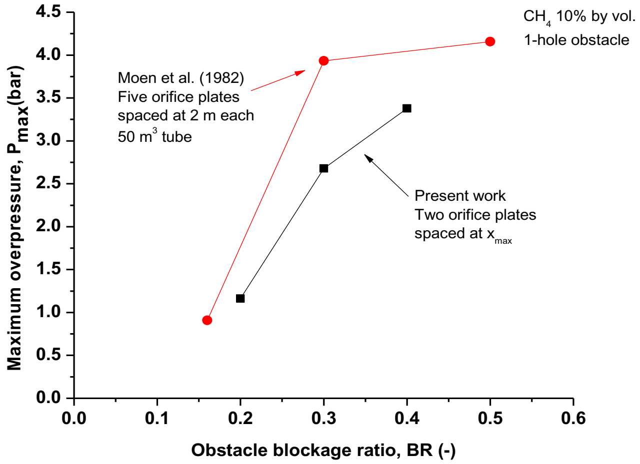

Fig. 7. Comparison between maximum overpressure and obstacle blockage for large scale [25] and present work.

3.3. Comparison with turbulent cold flow

A direct comparison between the intensity of turbulence in cold flow turbulence from [45] and maximum overpressure from the present work at different obstacle blockages is presented in Fig. 8. As noticed earlier, similar turbulence profile of growth, peak and decay were noticed in both cases. Also, the position to maximum explosion severity was found to decrease with increase in obstacle blockage. However, such positions occurred at a further distance than suggested in [45].

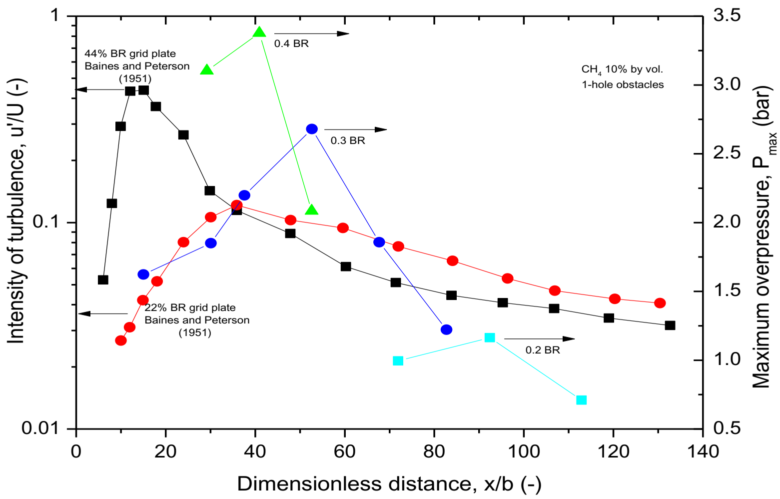

Fig. 8. Comparison between cold flow turbulence and transient flow experiments with different obstacle blockage ratios.

A possible explanation for the non-correspondence between the cold flow position of maximum turbulence and the worst case obstacle separation distance is that once the flame moves through the obstacle the whole of the generated turbulence profile is detached from the obstruction it is in fact conveyed forward (whilst at the same time being consumed) by the advancing flame front.

In the present work, the influence of obstacle separation was studied on various obstacle blockage ratios. In each case, an optimum spacing corresponding to the worst case explosion scenario was found. These spacing were then compared with multi-obstacle tests with fixed pitch from the literatures in order to quantify the effectiveness of obstacle spacing. Figures 9 and 10 show the relationship between dimensionless obstacle separation against maximum overpressure and flame speeds respectively.

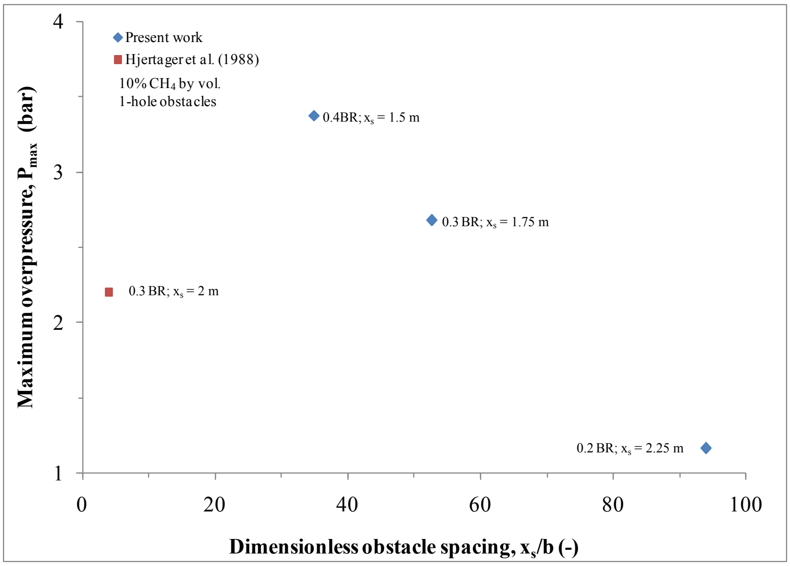

Fig. 9. Comparison between the present work and the literature on maximum overpressures and dimensionless obstacle spacing.

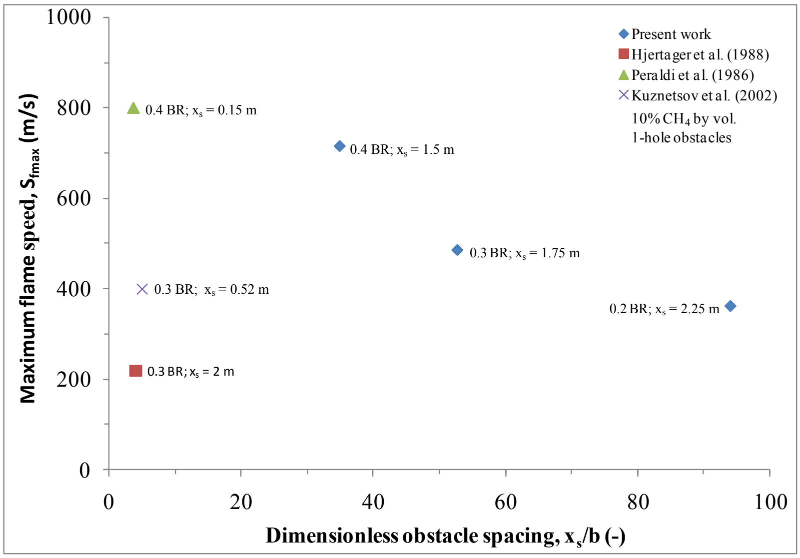

Fig. 10. Comparison between the present work and the literatures on maximum flame speeds and dimensionless obstacle spacing.

Table 2 shows an overview of the present test with optimum obstacle spacing and multi-obstacles from the literatures.

Table 2. Overview of explosion results on optimum obstacle spacing from the present work and multi-obstacles from the literatures.

Reference	Geometry	Gas	Conc.	BR	No	x_s	x_s/b	x to 1st obst.	P_{max}	S_{fmax}
(-)	(-)	(-)	(%)	(-)	(-)	(m)	(-)	(m)	(bar)	(m/s)
Present work	L = 4.25 m Ø = 0.162 m	CH_4	10	0.2	2	2.25	94	1	2.68	486
Present work	L = 4.25 m Ø = 0.162 m	CH_4	10	0.3	2	1.75	53	1	1.164	362
Present work	L = 4.25 m Ø = 0.162 m	CH_4	10	0.4	2	1.5	35	1	3.38	716
Peraldi*et al.* [10]	L = 18 m Ø = 0.15 m	CH_4	10	0.4	120	0.15	4	-	-	800
Hjertager*et al.* [8]	L = 10 m Ø = 2.5 m	CH_4	10	0.3	5	2	4	1.65	2.2	220
Kuznetsov*et al.* [56]	L = 34.5 m Ø = 0.52 m	CH_4	10	0.3	8	0.52	5	-	-	400

Wide-ranging series of experimental tests were carried out by [10] using three long tubes of 18 m long with the intention to establish quantitative limiting criteria for the onset of DDT. The internal diameter of each tube was taken to be 0.05, 0.15 and 0.3 m respectively. Fuels such as methane, propane, ethylene, acetylene and hydrogen of various concentrations ignited at the one end of the tube were used. The entire tube length was filled with orifice ring obstacles separated at one tube diameter apart. In comparison with the present work, 0.15 cm diameter tube was used. The authors attained a maximum flame speed of about 800 m/s for 10% methane-air by vol. with 0.4 BR. The flame speed value was just 1.12 times greater than that with two obstacles spaced at 1.5 m apart in the present work.

The present maximum flame speeds and overpressures with two 30% blockage obstacles were compared with those of [8]. These authors conducted their research in a vented large scale cylindrical tube of 50 m^3 by volume (10 m long and 2.5 m in diameter). Five 30% blockage steel rings were used as obstacles, regularly spaced at 2 m each apart. Various concentrations of either methane-air or propane-air homogeneously mixed were ignited with either planar or point source the closed end of the tube. For point ignition which is similar to the current work, the authors got a maximum overpressure and flame speed of slightly above 2 bar and 200 m/s respectively for 10% by vol. methane-air mixtures, compared to the significantly higher pressure of 2.7 bar and 486 m/s flame speed with just 2 obstacles of the same blockage but optimally spaced, in the present work.

The flame speeds from the current work were also compared with that of the extensive set of experimental data in obstacle laden tubes by [56]. The authors used a large scale tubular geometry of 34.5 m long and inner diameter of 520 mm equipped with 30% blockage orifice-plates spaced at one tube diameter. A flame speed of close to 400 m/s was attained for a slightly rich methane-air mixture at a distance similar to the length of the current explosion tube. This is nearly 100 m/s lower when compared to the 10% methane-air tests with just two obstacles spaced at 1.75 m in the present work.

The above comparisons clearly demonstrate the important effect the obstacle separation distance can have on the severity of the explosion and highlights the possibility that many previous studies with multi-obstacles may have under-demonstrated the effect of repeat obstacles. It was evident that the obstacle spacing from the literatures are quite closer (less than five obstacle scales) when compared to the present work. It can now be deduced that large congestions in a given medium do not necessarily signify potential maximum explosion severity as traditionally assumed. But, small congestions optimally separated apart could lead to devastating overpressure.

4. Conclusions

For both single and double obstacles, it was observed that an increase in obstacle BR from 0.2 to 0.4 resulted in increasing maximum overpressure and flame speeds. A maximum overpressure of about 1.7 bar and flame speeds of 370 m/s was attained from single 0.4 BR obstacle. For double obstacle of 0.4 BR optimally spaced, the maximum overpressure and flame speeds achieved doubled that of the single obstacle.

The positions to maximum overpressures and flame speeds were different with obstacle blockage. The highest obstacle blockage, 0.4 BR occurred at a shorter distance (35 obstacle scales) in comparison to 0.3 and 0.2 BRs which emerged at 53 and 94 obstacle scales respectively. This trend was similar to cold flow turbulence intensity of Baines and Peterson [45].

The positions to maximum overpressures and hence intensity of turbulence obtained for the 0.2-0.4 BRs in this work were in agreement with the cold flow prediction correlation of distance to maximum intensity of turbulence as given in Eq. 1 if multiplied by a factor of three.

It was evident that the obstacle spacing from the literatures is quite closer when compared to the present work. It can now be deduced that large congestions in a given medium do not necessarily signify potential maximum explosion severity as traditionally assumed. But, small congestions optimally separated apart could lead to devastating overpressure.

In planning the layout of new installations, it is appropriate to identify the relevant worst case obstacle separation in order to avoid it. In assessing the risk to existing installations and taking appropriate mitigation measures it is important to evaluate such risk on the basis of a clear understanding of the effects of separation distance and congestion. The present results would suggest that in many previous studies of repeated obstacles the separation distance investigated might not have included the worst case set up, and therefore existing explosion protection guidelines may not correspond to worst case scenarios.

Acknowledgements

The authors are thankful to the Nigerian Petroleum Technology Development Fund (PTDF) Overseas Scholarship Scheme, for supporting Abdulmajid Na'inna in his PhD studies on the subject.

References

[1] J.H.S. Lee, I.O. Moen, The mechans of transition from deflagration to detonation in vapor cloud explosions, Progress in Energy and Combustion Science, 6 (1980) 359-389.
[2] ATEX, ATEX (Explosive Atmosphere) Directives 94/9/EC, in, European Commission, 1994.
[3] W.R. Chapman, R.V. Wheeler, The propagation of flame in mixtures of methane and air. Part IV. The effect of restrictions in the path of the flame, Journal of the Chemical Society (Resumed), (1926) 2139-2147.
[4] W.A. Kirkby, R.V. Wheeler, Explosions in closed cylinders. Part V. The effect of restrictions, Journal of the Chemical Society (Resumed), Part V (1931) 2303-2306.
[5] H. Robinson, R.V. Wheeler, Explosions of methane and air: propagation through a restricted tube, Journal of the Chemical Society (Resumed), (1933) 758-760.
[6] R.K. Eckhoff, K. Fuhre, C.M. Guirao, J.H.S. Lee, Venting of turbulent gas explosions in a 50 m3 chamber, Fire Safety Journal, 7 (1984) 191-197.
[7] J.H.S. Lee, R. Knystautas, A. Freiman, High speed turbulent deflagrations and transition to detonation in H_2 air mixtures, Combustion and Flame, 56 (1984) 227-239.
[8] B.H. Hjertager, K. Fuhre, M. BjØRkhaug, Concentration Effects on Flame Acceleration by Obstacles in Large-Scale Methane-Air and Propane-Air Vented Explosions, Combustion science and technology, 62 (1988) 239-256.
[9] I.O. Moen, A. Sulmistras, B.H. Hjertager, J.R. Bakke, Turbulent flame propagation and transition to detonation in large fuel-air clouds, Symposium (International) on Combustion, 21 (1988) 1617-1627.
[10] O. Peraldi, R. Knystautas, J.H. Lee, Criteria for transition to detonation in tubes, Symposium (International) on Combustion, 21 (1988) 1629-1637.
[11] C.K. Chan, D.R. Greig, The structures of fast deflagrations and quasi-detonations, Symposium (International) on Combustion, 22 (1989) 1733-1739.
[12] D.J. Mackay, S.B. Murray, I.O. Moen, P.A. Thibault, Flame-jet ignition of large fuel-air clouds, Symposium (International) on Combustion, 22 (1989) 1339-1353.
[13] H.N. Phylaktou, Gas explosions in long closed vessels with obstacles : a turbulent combustion study applicable to industrial explosions, in: Fuel, University of Leeds, University of Leeds, 1993.
[14] V. Sakthitharan, Time-Resolved Measurements of Flame Propagation over Baffle-type Obstacles, in: Mechanical Engineering, University of London, University of London, 1995.
[15] C.K. Chan, W.A. Dewit, Deflagration-to-detonation transition in end gases, Symposium (International) on Combustion, 26 (1996) 2679-2684.
[16] S.B. Dorofeev, V.P. Sidorov, A.E. Dvoinishnikov, W. Breitung, Deflagration to detonation transition in large confined volume of lean hydrogen-air mixtures, Combustion and Flame, 104 (1996) 95-110.
[17] C.L. Gardner, Turbulent combustion in obstacle-accelerated gas explosions – The influence of scale, in: Fuel and Energy, University of Leeds, University of Leeds, 1998.
[18] V.I. Alekseev, M.S. Kuznetsov, Y.G. Yankin, S.B. Dorofeev, Experimental study of flame acceleration and the deflagration-to-detonation transition under conditions of transverse venting, Journal of Loss Prevention in the Process Industries, 14 (2001) 591-596.

[19] M. Kuznetsov, V. Alekseev, Y. Yankin, S. Dorofeev, Slow and fast deflagrations in Hydrocarbon-air mixtures, Combustion science and technology, 174 (2002) 157-172.
[20] B.J. Lowesmith, G. Hankinson, D.M. Johnson, Vapour cloud explosions in a long congested region involving methane/hydrogen mixtures, Process Safety and Environmental Protection, 89 (2011) 234-247.
[21] C. Dong, M. Bi, Y. Zhou, Effects of obstacles and deposited coal dust on characteristics of premixed methane–air explosions in a long closed pipe, Safety Science, 50 (2012) 1786-1791.
[22] V.N. Gamezo, R.K. Zipf, K.M. Mohamed, E.S. Oran, D.A. Kessler, DDT Experiments with Natural Gas-Air Mixtures, in: Proc. of the Seventh International Seminar on Fire & Explosion Hazards (ISFEH7), Research Publishing, Providence, Rhodes Island, 2013, pp. 729-738.
[23] H. Phylaktou, G.E. Andrews, The acceleration of flame propagation in a tube by an obstacle, Combustion and Flame, 85 (1991) 363-379.
[24] I.O. Moen, M. Donato, R. Knystautas, J.H. Lee, Flame acceleration due to turbulence produced by obstacles, Combustion and Flame, 39 (1980) 21-32.
[25] I.O. Moen, J.H.S. Lee, B.H. Hjertager, K. Fuhre, R.K. Eckhoff, Pressure development due to turbulent flame propagation in large-scale methane□ air explosions, Combustion and Flame, 47 (1982) 31-52.
[26] C. Chan, I.O. Moen, J.H.S. Lee, Influence of confinement on flame acceleration due to repeated obstacles, Combustion and Flame, 49 (1983) 27-39.
[27] A.J. Harrison, J.A. Eyre, The Effect of Obstacle Arrays on the Combustion of Large Premixed Gas/Air Clouds, Combustion science and technology, 52 (1987) 121-137.
[28] R.P. Lindstedt, H.J. Michels, Deflagration to detonation transitions and strong deflagrations in alkane and alkene air mixtures, Combustion and Flame, 76 (1989) 169-181.
[29] A. Teodorczyk, J.H.S. Lee, R. Knystautas, Propagation mechanism of quasi-detonations, Symposium (International) on Combustion, 22 (1989) 1723-1731.
[30] W.P.M. Mercx, Large-scale experimental investigation into vapour cloud explosions: comparison with the small-scale Discoe trials, Institution of Chemical Engineers, 70 Part B (1992) 197-204.
[31] R. Beauvais, F. Mayinger, G. Strube, Severe Accident in a light water reactor: Influence of elevated initial temperature on hydrogen combustion, ASME/JSME Nuclear Engineering Conference, 1 (1993) 425-433.
[32] T. Obara, S. Yajima, T. Yoshihashi, S. Ohyagi, A high-speed photographic study of the transition from deflagration to detonation wave, Shock Waves, 6 (1996) 205-210.
[33] V.V. Mol'kov, V.V. Agafonov, S.V. Aleksandrov, Deflagration in a vented vessel with internal obstacles, Combust Explos Shock Waves, 33 (1997) 418-424.
[34] L.X. Yu, W.C. Sun, C.K. Wu, Flame acceleration and overpressure development in a semiopen tube with repeated obstacles, Proceedings of the Combustion Institute, 29 (2002) 321-327.
[35] G. Ciccarelli, C.J. Fowler, M. Bardon, Effect of obstacle size and spacing on the initial stage of flame acceleration in a rough tube, Shock Waves, 14 (2005) 161-166.
[36] A. Teodorczyk, P. Drobniak, A. Dabkowski, Fast turbulent deflagration and DDT of hydrogen–air mixtures in small obstructed channel, International Journal of Hydrogen Energy, 34 (2009) 5887-5893.
[37] W. Rudy, R. Porowski, A. Teodorczyk, Propagation of hydrogen-air detonation in tube with obstacles, Journal of Power Technologies, 91 (2011) 122-129.
[38] K.G. Vollmer, F. Ettner, T. Sattelmayer, Deflagration-to-detonation transition in hydrogen-air mixtures with concentration gradients, in: 23rd International Colloquium on Dynamics of Explosions and Reactive Systems (ICDERS), Irvine, 2011.
[39] L. Pang, Q. Zhang, T. Wang, D.C. Lin, L. Cheng, Influence of laneway support spacing on methane/air explosion shock wave, Safety Science, 50 (2012) 83-89.
[40] L.R. Boeck, J. Hasslberger, F. Ettner, T. Sattelmayer, Investigation of Peak Pressures during Explosive Combustion of Inhomogeneous Hydrogen-Air Mixtures, in: Proc. of the Seventh International Seminar on Fire & Explosion Hazards (ISFEH7), Research Publishing, Providence, Rhodes Island, 2013, pp. 959–965.
[41] R. Porowski, A. Teodorczyk, Experimental study on DDT for hydrogen–methane–air mixtures in tube with obstacles, Journal of Loss Prevention in the Process Industries, 26 (2013) 374-379.
[42] W.P.M. Mercx, D.M. Johnson, J. Puttock, Validation of scaling techniques for experimental vapor cloud explosion investigations, Process Safety Progress, 14 (1995) 120-130.
[43] A.M. Na'inna, H.N. Phylaktou, G.E. Andrews, The acceleration of flames in tube explosions with two obstacles as a function of the obstacle separation distance, Journal of Loss Prevention in the Process Industries, 26 (2013) 1597-1603.
[44] A.M. Na'inna, H. Phylaktou, G.E. Andrews, Acceleration of Flames in Tube Explosions with Two Obstacles as a Function of the Obstacle Separation Distance: The Influence of Mixture Reactivity, in: Proc. of the Seventh International Seminar on Fire and Explosion Hazards (ISFEH7), Research Publishing, Providence, USA, 2013, pp. 627-636.
[45] W.D. Baines, E.G. Peterson, An investigation of flow through screens, Trans. American Society of Mechanical Engineering, 73 (1951) 167.
[46] G.F. Robinson, A.A. Kovitz, AAIA J., 13 (1975).
[47] M.D. Checkel, Turbulence enhanced combustion of lean mixtures, in, University of Cambridge, University of Cambridge, 1981.
[48] J. Tan-Atichat, H.M. Nagib, R.I. Loehrke, Interaction of free-stream turbulence with screens and grids: a balance between turbulence scales, Journal of Fluid Mechanics, 114 (1982) 501-528.
[49] J. Groth, A.V. Johansson, Turbulence reduction by screens, Journal of Fluid Mechanics, 197 (1988) 139-155.
[50] R.E. DeOtte Jr, G.L. Morrison, D.L. Panak, G.H. Nail, 3-D laser Doppler anemometry measurements of the axisymmetric flow field near an orifice plate, Flow Measurement and Instrumentation, 2 (1991) 115-123.
[51] D.W. Zhou, S.-J. Lee, Heat transfer enhancement of impinging jets using mesh screens, International Journal of Heat and Mass Transfer, 47 (2004) 2097-2108.
[52] H.N. Phylaktou, G.E. Andrews, Prediction of the maximum turbulence intensities generated by grid-plate obstacles in explosion-induced flows, Symposium (International) on Combustion, 25 (1994) 103-110.
[53] A.T. Cates, S.J. Bimson, Fuel and obstacle dependence in premixed transient deflagrations, in: 13th International Colloquium on Dynamics

of Explosions and Reactive Systems (ICDERS), ICDERS, Nagoya University, Japan, 1991.
[54] M. Bjorkhaug, Flame acceleration in obstructed radial geometries, in, City University London, London, 1986.
[55] D. Yibin, X. Fuquan, X. Xiaoyan, C. Xin, D. Hongbin, Investigation of solid structure obstacles influence on flame propagation in semi-open tube, Procedia Engineering, 26 (2011) 538-544.
[56] M. Kuznetsov, G. Ciccarelli, S. Dorofeev, V. Alekseev, Y. Yankin, T.H. Kim, DDT in methane-air mixtures, Shock Waves, 12 (2002) 215-220.